J. Fluid Mech. (1970), *vol.* 40, *part* 3, *pp.* 453–479
Printed in Great Britain

The flow created by a sphere moving along the axis of a rotating, slightly-viscous fluid

By T. MAXWORTHY

Geophysical Fluid Dynamics Laboratory,
University of Southern California, Los Angeles

(Received 26 December 1968)

The title flow has been studied by measuring the drag force on, and by observing the flow field around, a sphere rising through a large, rotating tank of water. Long, almost stagnant, regions are formed up- and downstream within the shadow of the sphere and are surrounded by a thin annular region within which the velocity is larger than the mean velocity of the approach flow. Several regions are found within which vortex-jump phenomena occur and it is concluded that such features exert a controlling influence over the dynamics of the observed flow field.

1. Introduction

We reconsider a problem originally outlined by Proudman (1916) and by Taylor in a series of papers published between (1917) and (1923), and look in detail at the flow created by a body as it moves along the axis of a long, rotating tank of water.

By now it is well known that rotation introduces many novel features into the possible motions of a fluid. An extensive study has recently been published by Greenspan (1968). Of particular interest in this work are: (*a*) the ability of a rotating, incompressible fluid to support circularly polarized wave motions that propagate along the rotation vector; (*b*) a resistance to motions across the externally applied vortex lines, i.e. a Coriolis force acting on fluid particles as they try to move radially; (*c*) the appearance of various secondary motions, usually associated with the boundary layer or shear layers required to match a region of rotating flow to a solid surface or adjacent fluid region rotating at a different rate. The existence of these effects require considerable additions to our intuition before we can construct even the general character of the flow field produced by a particular rotating geometry.

An excellent example of the need to modify our previous intuition occurs in the present case, for within its very simple framework exists a bewildering variety of curious phenomena. The basic phenomenon was discovered, experimentally, by Taylor (1922). He found that as a sphere moved slowly† through a fluid in basic solid-body rotation, a column of fluid was pushed ahead of the sphere as a 'slug'

† The real meaning of the adverb slowly will appear later when it is possible to attach some quantitative measure to it (§ 4, figures 11, 12).

of zero axial velocity, relative to the body. In the limit of zero viscosity this column was presumed to become a cylinder, extending ahead and behind the body, with generators parallel to the axis of rotation and just touching the largest cross-section of the body. What he saw has been presumed to be the viscous modification of the ideal flow. Taylor reported that this behaviour appeared only when the parameter $N = 2\Omega a/U_\infty$† exceeded a magnitude of about 6. Here Ω is the angular velocity of the solid-body rotation, U_∞ and a are the velocity and radius of the sphere, respectively. No cylindrical flow was seen behind the body.

Further observations by Long (1953) demonstrated the existence of a train of waves downstream of the disturbing body when N was small. They apparently disappeared as N approached the slug-flow régime. Again, there were visualizations of slug flow ahead of the body and of a strong, cyclonic vortex behind.

The questions that arose in reading these accounts and the reviews of more recent years (Squire 1956, Greenspan 1968) were first tested, by the writer, in a very simple rotating-tank apparatus. Several curious inconsistencies were found. The existence of the forward slug was verified, but it did not disappear when N was less than 6. It was much in evidence for values around 2, but in a modified form. Under no circumstances was the axial velocity within the slug zero, although it was very much smaller than U_∞. A rearward slug was observed at large N. For small values of N it rotated rapidly, had an oscillatory character, was much longer than the forward slug and completely modified the separation bubble that normally exists at the Reynolds numbers of the experiments.

A more detailed experimental programme was carried out in order to understand these and other features of the flow. The study can be divided into several fairly distinct parts. In § 3, we consider the drag force experienced by a sphere as it rises through a rotating, viscous fluid. These measurements point to certain interesting regions of flow, which are studied in more detail in § 4. Here observations of the velocity fields are presented, together with certain objections that might be raised to the interpretation of these observations. Section 5 has been added in an attempt to answer the more obvious of these difficulties.

Taken by themselves these results have significance, for they tell a great deal about possible motions in a rotating system. They have added significance when their similarity to magneto-fluid dynamic and stratified fluid flows is considered. In fact, this similarity was one of the main reasons for performing the present experiments and led to considerable insights into the similar, but inaccessible, magneto-fluid dynamic flow (Maxworthy 1968*a*).

Several authors have added to our theoretical knowledge of the subject. Of necessity, their work is of limited applicability because of the strict assumptions needed to make the problem tractable.

We start with the limiting case of a steady, inviscid flow. Taylor (1922) discovered the basic inconsistency of such a limit. There are insufficient boundary conditions to determine the flow completely, and one is forced to make suitable assumptions to remove the degeneracy. Taylor gave a particular solution for

† $2\Omega a/U_\infty$ measures the relative magnitude of Coriolis to inertia forces or inertial wave propagation speed to convection speed.

which *all* the velocity components at the body are zero in this *inviscid* flow! More recently, various authors have chosen to attack this difficult problem in a variety of ways. Stewartson (1952) used a Laplace transform technique and considered how the inviscid flow, for large N, could be produced by an impulsively started body, a problem that had been partially solved by Grace (1926) using a power-series expansion in time. Morrison & Morgan (1956), Childress (1962 and private communication) and, more recently, Moore & Saffman (1969) consider a steady flow but include viscosity and take the limiting flow as T and $R \to \infty$, with $N = 2T/R$ remaining finite but large; where T, the Taylor number, is $\Omega a^2/\nu$ and R, the Reynolds number, is $U_\infty a/\nu$; ν is the kinematic viscosity of the fluid. Bretherton (1967) has studied the impulsive motion of a cylinder in a viscous fluid in considerable detail. He showed how high-frequency inertial waves are preferentially damped while the longer wavelengths propagate further and ultimately produce disturbances far from the body. The picture that emerges from these studies is sketched in figure 1. Stagnant rotating regions extend a distance $O(T)$ up- and downstream. These are matched to the outer flow by a shear layer of $O(T^{-\frac{1}{3}})$ in thickness and to the body by an Ekman boundary layer of thickness $O(T^{-\frac{1}{2}})$. All these studies predict a drag coefficient $C_D = 1{\cdot}71N$,

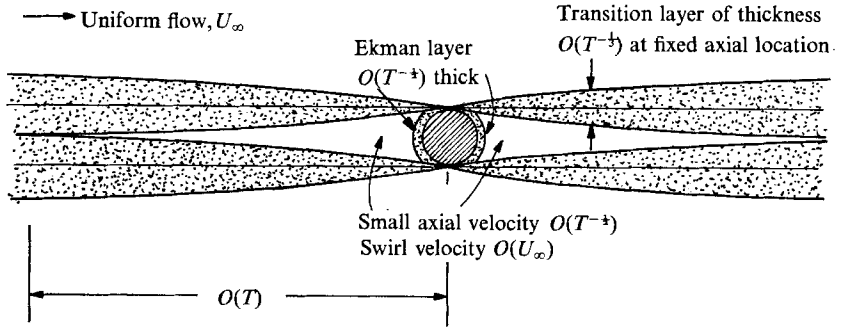

FIGURE 1. Sketch of linear theoretical model of the flow at large T and N.

where C_D is the conventional drag coefficient: drag/$\frac{1}{2}\rho U_\infty^2 \pi a^2$, where ρ is the fluid density. No attempt has been made to calculate the more complicated interaction problem defined when the effect of the Ekman boundary-layer flux on the outer flow is to be found. It is well known that such effects are of great importance in rotating flows (Rott & Lewellen 1966), but they are not sufficiently well understood to allow a quantitative, or even qualitative, extension to the present case.

Long (1953) removed the non-uniqueness by allowing the body to move in a tube of finite radius and used the boundary conditions at the tube wall to give the required, extra condition. In this way, he was able to predict, and in fact observe, the existence of a set of standing waves behind the body for $T \gg 1$ and $N = O(1)$.

Stewartson (1958) and Miles (1969*a*, *b*) have calculated the inviscid flow around a sphere and the latter the inviscid flow about a slender ellipsoid of revolution under the assumption of no upstream wave propagation and N not

large. These results have some bearing on the experimental observations and further comments are postponed until § 4.2.

Childress (1964) presented a solution for a very viscous fluid, i.e. R and $T \to 0$, with $R/T^{\frac{1}{2}}$ remaining finite, but this is not an appropriate limit for the present case, except far up- and downstream.

When judiciously chosen, *a posteriori*, these theories have some of the features encountered in the experimental flows. Unfortunately, the range of parameters over which any one of the theories applies is usually quite limited and in some cases cannot even be reached.

2. Apparatus and experimental techniques

Basically, the system consists of a rotating cylinder of water through which a body can move.

The details of this simple system are shown in figures 2 and 3. A Lucite cylinder is supported, axially, on a tapered-roller bearing and transversely by a 'steady-rest', consisting of three rubber-tyred wheels. All of these bearings are fixed

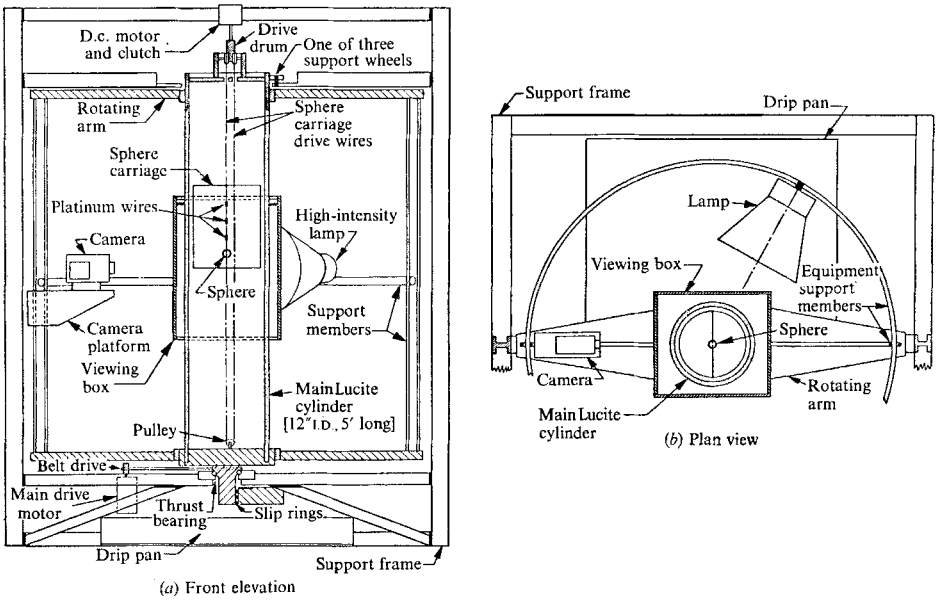

FIGURE 2. Details of the rotating-tank apparatus with pulley system, used to tow a sphere and hydrogen-bubble wire, installed.

to a massive angle-iron frame, which is the main supporting structure for the whole apparatus. Two light aluminium arms are clamped to the cylinder, and a large ring, of 4 ft. diameter, is attached to them. The ring and arms serve as support for a camera, light source and any other peripheral equipment that might be required. A system of slip rings is machined into the brass base of the large cylinder and connects the various internal electrical devices to the external power supplies. The latter supply power to the lights, to the shutter mechanism of the camera, or to the drive motor of the moving picture camera when it is used.

In order to eliminate optical distortion in the test area, due to the lens effect of the cylindrical air/Lucite/water interface, it was surrounded over a 24 in. length by a rectangular box filled with water, indicated as 'viewing box' in figure 2.

Different pieces of test apparatus could be introduced into this basic rotating system for the following purposes:

2.2. *Sphere drag measurements*

A device to release a freely rising sphere in order to measure its time of flight through the tank, and hence its drag, is shown in figure 3(*a*). It consisted of a multi-barrelled magazine, to hold several spheres, which could be moved, through a system of wires and pulleys, from outside the rotating tank. Each sphere was backed by a weak spring, and as it was brought into position below the single exit hole, the sphere would spring free and continue its rise unimpeded.

The actual measurement of sphere drag is a simple modification of the technique used in Maxworthy (1965). Twelve $\frac{1}{2}$ in. diameter and eight $\frac{3}{4}$ in. diameter polypropylene spheres were plated with a thin coating of copper. By carefully controlling the removal of some of the copper in a nitric acid bath, a sphere could

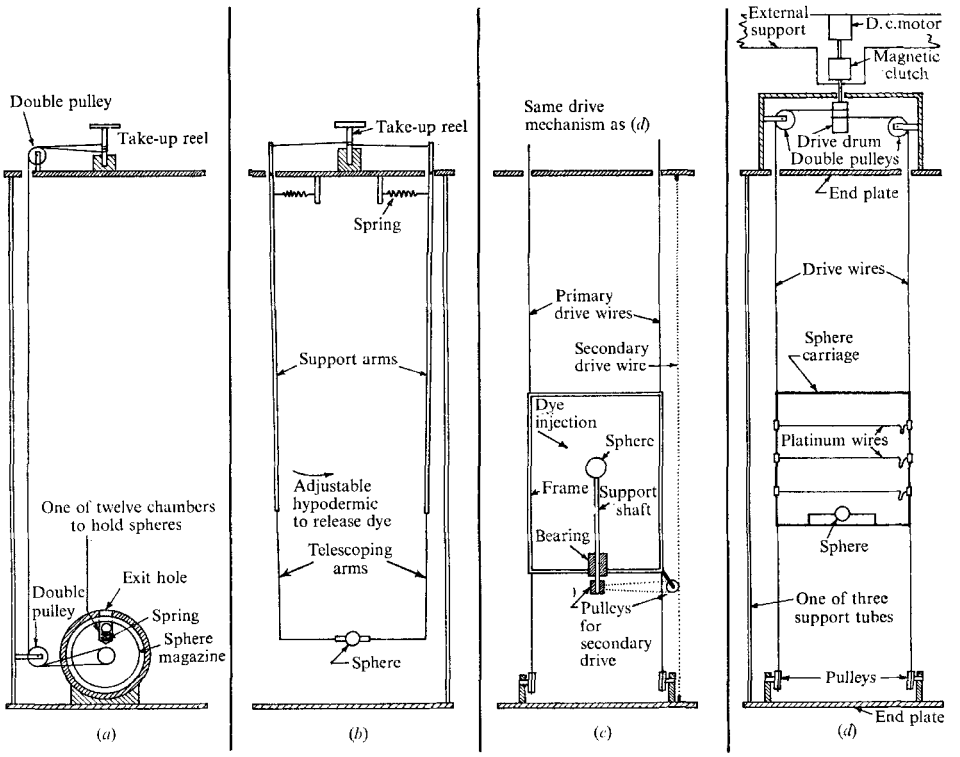

FIGURE 3. Various pieces of equipment that could be lowered into the basic rotating tank apparatus to perform the following tasks: (*a*) release a series of buoyant spheres from the bottom of the tank; (*b*) release a single sphere from the centre of the tank; (*c*) tow a sphere along axis of the tank and rotate it at a rate independent of the basic rotation rate; (*d*) tow a sphere and hydrogen-bubble wires along the axis of the tank.

be produced that would rise at approximately the desired speed in a tank of water. In this fashion, a series of spheres was made which rose at velocities between 7 cm/sec and 0·5 cm/sec. Each sphere was given an identifying mark.

The spheres were placed in the magazine of the sphere-release mechanism of figure 3(*a*), and the whole framework lowered into the stationary tank. When all random fluid motion had ceased, the spheres were released in turn and their time of flight measured. The magazine was reloaded, the whole tank set into rotation, and the time of rise measured again. Runs with and without rotation were made alternately until the full range of rotation parameter had been covered. Since we assume that the curve of drag coefficient (C_D) *versus* Reynolds number is known with no rotation, runs with no rotation measure the buoyancy force acting on the sphere. When the same sphere rises through the rotating fluid, its buoyancy force is the same, but its time of flight and hence its R and C_D are changed. Thus, by multiplying the calibration drag coefficient by the square of the inverse ratio of the rise times, we obtain the drag coefficient with rotation, and by multiplying the calibration R by the ratio of the rise times, we obtain R with rotation.

2.3. *Flow field observations*

Several methods were used for qualitatively and quantitatively observing the flow field due to the sphere motion. Dye injection gave a first crude picture of the over-all flow pattern, and then the hydrogen-bubble technique was used to give a better quantitative picture of certain detailed properties of the velocity field. Since several different modifications of these techniques were used, each will be described in detail.

Dye studies in the apparatus of figure 3(*b*) will be considered first. The sphere was started in a region of high dye concentration and rose into a region of clear water. It dragged with it dye trapped in regions where the fluid was moving with essentially the sphere velocity. This method showed up the almost stagnant regions in front of and behind the body as well as some details of the flow in the boundary layers around the sphere, e.g. (figures 8, 9*a*, *b*). A sphere was released above or below a region of dyed fluid, in order to study the transient growth of the stagnant regions.

If small amounts of dye were introduced into the test section slightly before solid body rotation had been achieved, they were drawn out into thin sheets wrapped around the axis of rotation. These so-called 'Taylor-walls' essentially marked stream surfaces in the undisturbed fluid. If a sphere was allowed to rise through the centre of the region of marked stream surfaces, they were distorted in such a way that they still represented stream surfaces, but then of the flow about the body.

Figure 3(*c*) shows a towed sphere that could be rotated independently of the basic speed of rotation of the whole system. The sphere was mounted on a support shaft which in turn rotated in a Teflon bearing. This bearing was rigidly attached to a heavy wire frame which moved up and down in the same manner as the frame in figure 3(*d*). In order to rotate the sphere independently, a secondary drive wire was attached at its two ends to the brass end-plates; it also passed over

a double pulley attached to the frame and a secondary drive pulley mounted on the support shaft. As the carriage moved up and down, the secondary drive wire was pulled through the pulley system and rotated the sphere at a rate that depended on the velocity of the sphere, once the geometrical factors had been fixed. This apparatus was used to observe the nature of the forward disturbance. The reasons for its use are discussed in § 4.2.

Dye observations were invariably lit from behind, the illumination falling on a translucent screen taped to the back of the viewing box.

Finally, for quantitative velocity measurement we needed a mechanism to tow a sphere and some type of measuring instrumentation through the flow. It is this equipment which is shown installed in figure 2 and in further detail in figure 3(*d*). It is supported within the Lucite cylinder by two brass end-plates rigidly connected by three stainless-steel tubes. Two continuous, stainless-steel drive wires, running in a system of grooved, free-running pulleys, supported a heavy wire frame, on which the sphere was mounted. Sphere and carriage could be traversed up and down, from outside the rotating system, by turning the drive drum from a variable speed d.c. motor through a magnetic clutch. The latter was incorporated so that drive motor and drive drum could be disconnected. When disconnected, the drum would rotate at the same speed as the main system and the sphere be brought to rest.

The hydrogen-bubble technique was used in this study and has been described by Schraub *et al.* (1965). With care, it can be used to give reasonably accurate quantitative measurements of velocity and a qualitative picture of the flow character. It was chosen in the present situation for several reasons. Disturbances due to the presence of the small wire were themselves small; the flow velocities were low enough for most conventional techniques to be quite inadequate; the difficulty of bringing electrical information out of the rotating system made photography of hydrogen-bubble lines particularly attractive. The technique can be used in any of several ways.

By stretching a thin, bare platinum wire across a diameter in the flow ahead of the body and viewing the motion of the hydrogen bubbles as they were removed from the wire, two of the three velocity components, in a rotating co-ordinate system, could be determined. When a front elevation of the bubbles was viewed, the radial distribution of axial velocity $\tilde{v}_x(\tilde{r})$† could be found. If a plan view was taken, the radial distribution of swirl velocity $\tilde{v}_\theta(\tilde{r})$ could be measured.

Because of geometric limitations, the latter method could not be used and the following, more convenient alternative substituted. With respect to the wire, the fluid and hence the line of bubbles were both moving axially and rotating (radial motion was assumed small for the times considered). In principle, by pulsing the wire twice and forming two lines of bubbles at different times, it was possible to extract both velocity profiles. Actually, such a method was not very accurate and it was necessary to form many lines of bubbles closely spaced in time and space in order to improve the accuracy. The method is more precisely

† $\tilde{v}_i$ are the components of the velocity vector in a cylindrical rotating, co-ordinate system, $\tilde{x}$, $\tilde{r}$, θ. $\tilde{\omega}$ is the angular velocity, i.e. $\tilde{v}_\theta = \tilde{\omega}\tilde{r}$. Superscript $\sim$ refers to dimensional quantities.

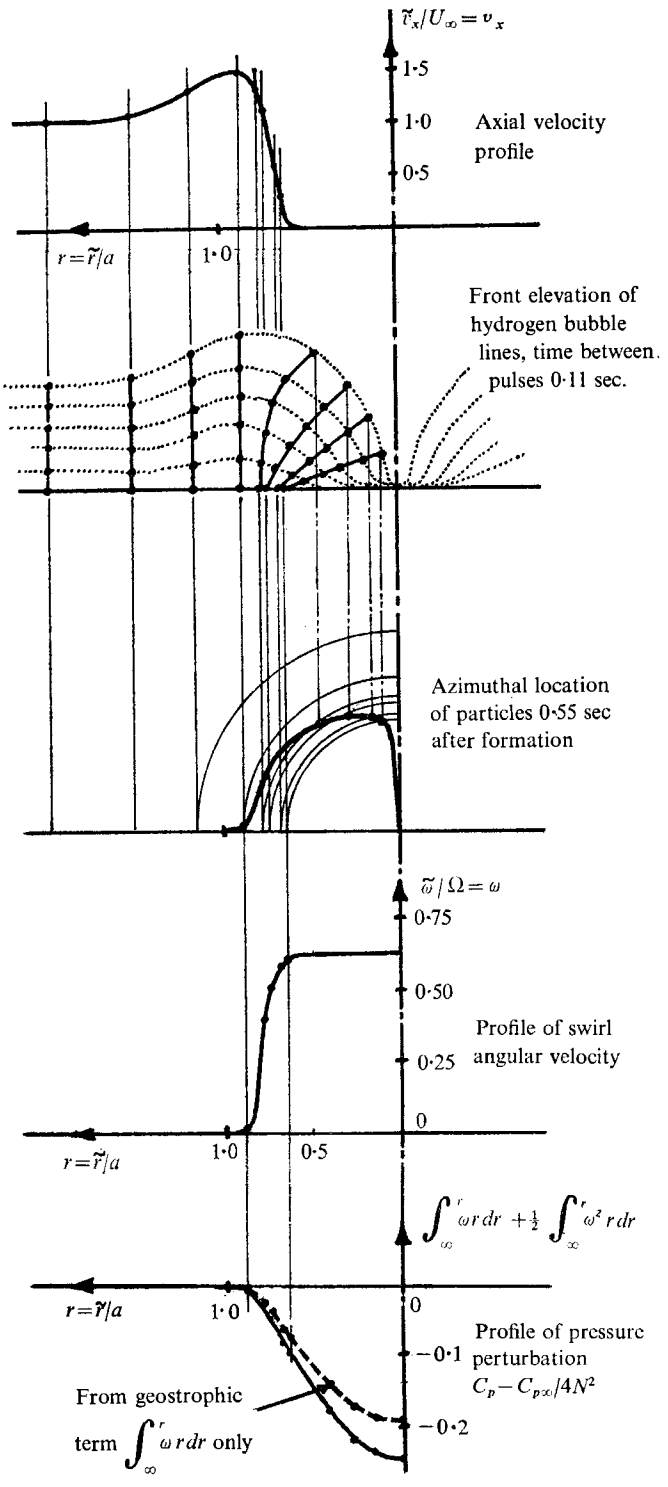

FIGURE 4. Illustration of the method used to extract velocity information from hydrogen-bubble lines which are being both rotated and moved axially. Rearward wake four sphere radii downstream of sphere. $N = 7{\cdot}86$, $T = 390$.

illustrated in figure 4, where a tracing from an actual experiment is shown; a photograph is shown in figures 9(*c*) and 18(*b*) for a different experiment. The time interval between each pulse is $\Delta t = 0{\cdot}11$ sec, and distance is referred to the sphere radius, which is 0·952 cm. The axial distance (Δx), moved by a hydrogen bubble with axial velocity $\tilde{v}$, is given by $\Delta\tilde{x} = \tilde{v}\,.\,\Delta t(n+m)$, where n is the integral number of pulses from the initial pulse and m is a quantity which represents the fraction of Δt which has passed since the last pulse was created and the photograph was taken. For given $\tilde{v}$, $\Delta\tilde{x}$ is found for each of the pulses present and the location marked; these marked points are joined by a smooth curve and extrapolated to zero time. This point represents the radial location with the chosen $\tilde{v}$. Any apparent radial displacement of this point from its extrapolated position is due to rotation of the line of particles. Once the true radial location of a series of different velocities ($\tilde{v}$) is known, we can determine the azimuthal location of a particle by knowing its starting position and its radial location at some later time, and use the geometrical construction shown in figure 4.

The radial velocity component is difficult to measure with any wire orientation and must be inferred either from the other velocity components, using the continuity equation, or from the orientation of flow streamlines.

The streamline patterns themselves can be found by coating the platinum wire with a suitable insulator, leaving only small bare sections at appropriate intervals. As the wire and body move through the tank, the hydrogen-bubble trail is left behind to form a streamline, if the flow is steady, and unsteady streakline otherwise. Alternatively, they can be found by using the dyed stream-tube method described previously, or by continuity of the axial volume flux.

Finally, some idea of the three-dimensionality of the flow can be gained by running a bare wire with a continuous current. Distortions of the sheet of bubbles so formed indicate in a useful way the three-dimensionality of the wakes.

Contrast between the hydrogen bubbles and the dark background was greatest when illuminated by the high-intensity lamp directed at about 110–120° from the line of view of the camera, as shown in figure 1.

In most cases the information was recorded photographically, using either a 35 mm framing camera or a 16 mm ciné camera. The latter was used as a substitute for direct visual observation, which proved to be difficult for a stationary observer viewing flow in a rotating system. It showed, initially, an oscillation of the basic solid body rotation which had not been suspected. Removal of these oscillations required a very careful realigning and balancing of the whole system to prevent oscillatory motions of the rotating tank, which were transferred to the rotating fluid through motions of the free surface, as discussed by Fultz in Küchemann (1965).

3. Results of sphere drag measurements

These are shown graphically on figures 5 and 6, where they are plotted to facilitate comparison with conventional sphere-drag results with no rotation (figure 5) and so as to bring out the simple dependence on N when T and N are large (figure 6). Interpolation with the results of Maxworthy (1965), for drag

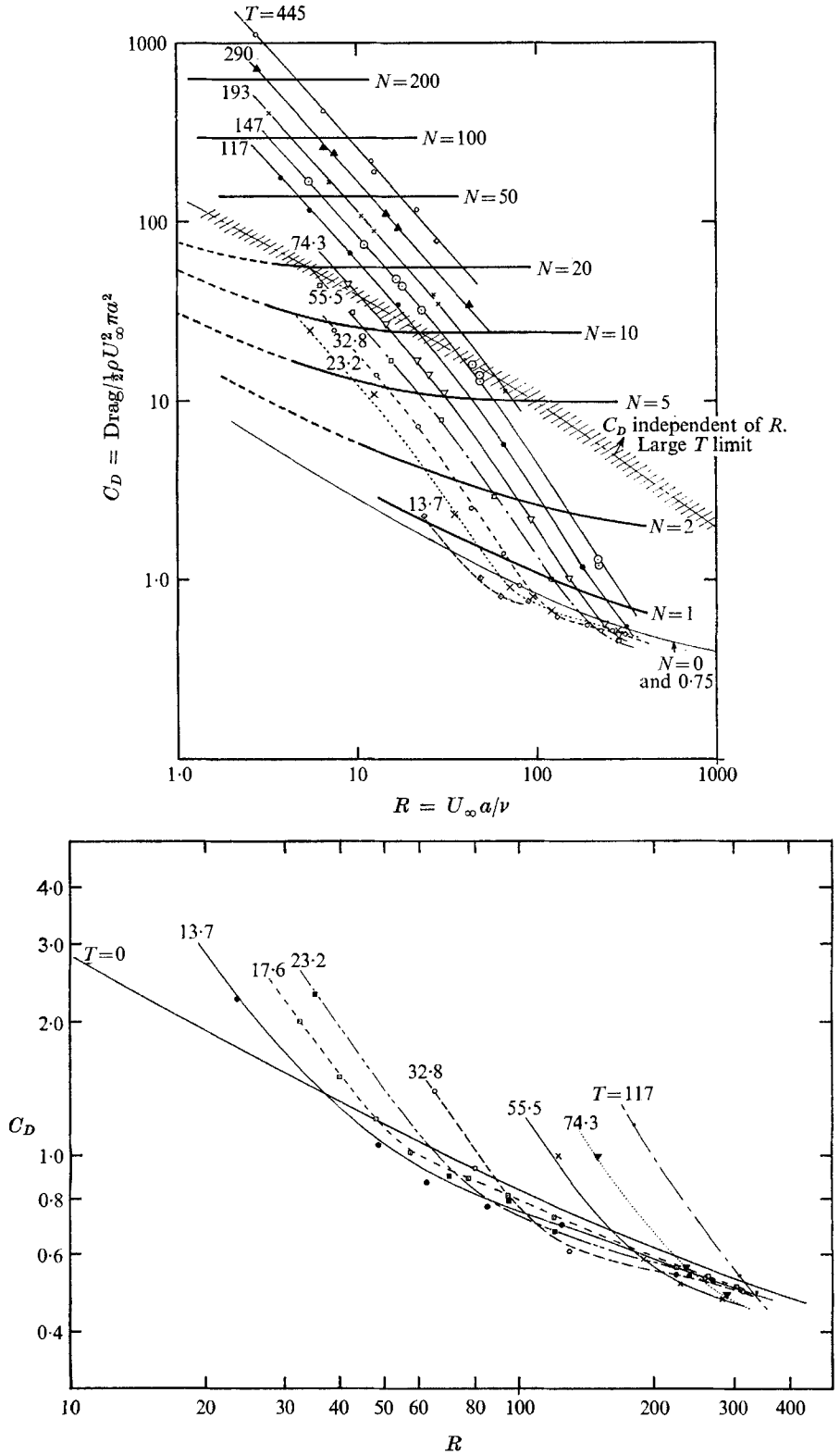

FIGURE 5. Drag coefficient (C_D) *versus* Reynolds number (R) with interaction parameter (N) and Taylor number (T) as parameters.

at very low R, has been used to extend the present results to lower R than the actual experiments. Several interesting features should be noted:

(i) At low N the drag is *less than the drag with no rotation*; this occurs in the range $O < N < 0{\cdot}75 \pm 0{\cdot}03$, independently of T (cf. the results of Stewartson 1968). Such a result can be explained physically by considering a weakly rotating fluid flowing over the sphere plus a rear recirculation region similar, in shape,

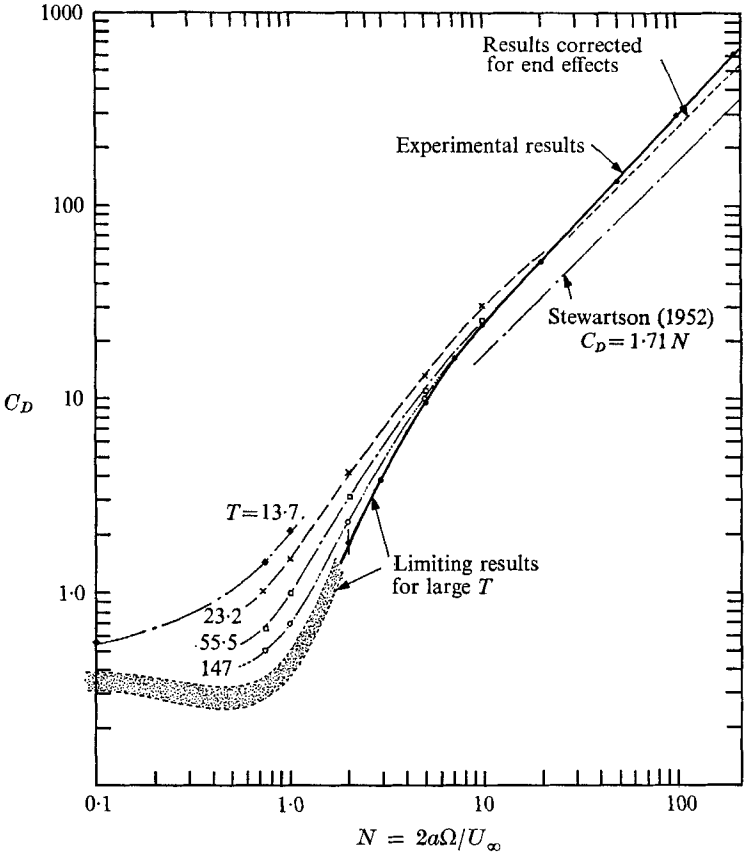

FIGURE 6. Drag coefficient (C_D) *versus* interaction parameter (N) with Taylor number (T) as parameter. See text for explanation of the shaded region.

to that in a non-rotating fluid, i.e. viscous separation takes place before the equator and the bubble has a larger transverse dimension than the sphere. The outward flow of rotating fluid over this bubble causes it to rotate at a rate less than the applied value, the pressure in the bubble increases, and the drag on the body decreases.

(ii) For large T the drag coefficient depends only on N. The value of N at which this first occurs is a function of T given approximately by $N = 1{\cdot}4 \times 10^2 T^{-\frac{1}{3}}$.

In the present apparatus, for which $2a/L = 0{\cdot}013$ (where L is the length of the tank), for large T and for large enough values of N,

$$C_D \sim N^{1{\cdot}07}.$$

The results of Maxworthy (1968*b*), for which $2a/L = 0{\cdot}215$, and some unpublished results of Fultz, can be used to extrapolate the present results to those for an infinitely long cylinder. Then, for large T and N,

$$C_D = AN^B,$$

where $A = 2{\cdot}60 \pm 0{\cdot}05$; $B = 1{\cdot}00 \pm 0{\cdot}01$, which is to be compared with the inviscid calculation of Stewartson (1952) and others, in which $C_D = 1{\cdot}71N$. Here we must introduce an interesting coincidence for which there is no rational explanation at the moment. Moore & Saffman (1969) repeated the viscous calculations of Morrison & Morgan (1956) and Childress (1962) using a simpler method. When they extended the calculation, using 'a boundary-layer approximation to the viscous stresses and the equation of continuity', they obtained a drag coefficient equal to $2{\cdot}67N$, which is only $2\frac{1}{2}$ % greater than the measured value!

It seems unlikely that the drag should depend on the presence of the cylindrical walls, as detailed in Maxworthy (1965), although this possibility must not be overlooked in certain ranges of parameters where Long's (1953) arguments are valid, and only a few inertial wave-numbers are excited. Results for $\frac{1}{2}$ in. and $\frac{3}{4}$ in. diameter spheres were identical in the region of parameter space in which they overlapped.

(iii) For very large T ($> 10^3$) and for a small range of N between 1·4 and 4,

$$C_D = 4{\cdot}10N^{2{\cdot}00}.$$

Data for this range was obtained with reasonable certainty ($\pm 0{\cdot}02$) by extrapolating the results at the experimental values of R to higher values. The shaded results on figure 6 below $N \approx 2$ are a guess based on the known constant values of C_D for $N = 0$ and the measured behaviour of C_D at smaller values of T, i.e. the observation that the drag coefficient with rotation is smaller than the value with no rotation, by a maximum of about 0·04 at large R. In fact, the maximum drag decrease divided by the value at $N = 0$ has a constant magnitude of 0·135 for the experiments reported.

(iv) For intermediate ranges of T and N the drag is greater than the drag with no rotation, but does not exhibit any convenient dependence on the parameters over large variations in their values.

These results point to interesting regions in parameter space, which are investigated in greater detail in the following sections. In particular, the results at large T and N exhibit such a simple drag law that the flow should have some features that are amenable to simple physical and mathematical interpretation.

A by-product of these free-rise measurements are some observation on the dynamical behaviour of the spheres as they rose through the tank. When N was large, the sphere rotated at the same rate as the tank. As N was decreased below about 5, the sphere began to rotate at a slower rate until at N around unity it was not rotating at all in the laboratory frame of reference (cf. Taylor 1922). The transition from full rotation to no rotation took place rapidly, almost discontinuously (see § 4 for the comparable behaviour of the lengths of the 'Taylor columns').

4. Results of flow field observations

4.1. *General features of the flow field*

Attempting to describe the flow field is a difficult task because of the wealth of detail that exists even in the simpler limiting case of large T and N. Since the flow field also changes as the parameters vary from this case, the construction of a simple, logical picture is virtually impossible.

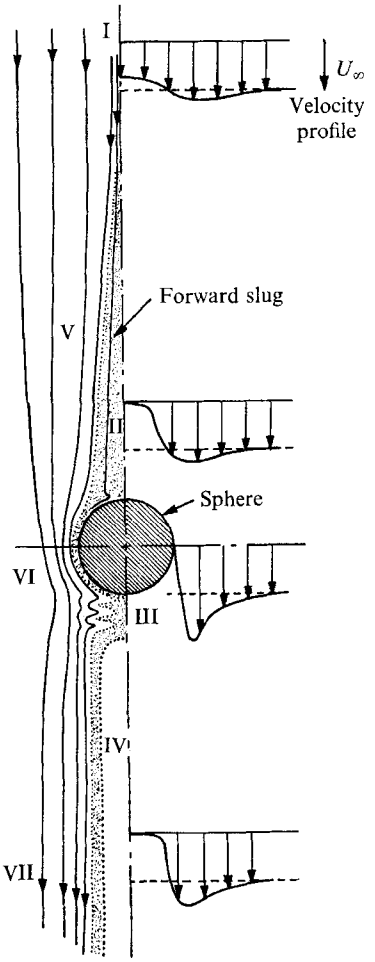

FIGURE 7. Sketch of the flow around a sphere moving through a rotating fluid. Roman numerals refer to regions of the flow considered in detail in the text.

We start our attempt with figure 7, which shows features that are common to the majority of the cases studied. It is biased towards the type of flow that is more typical of large values of N; flows at small N are different in detail, not in general, qualitative features. Meridional streamlines are shown, together with axial velocity profiles. The shading indicates the almost stagnant region as shown by dye studies (figure 8, plate 1, and figures 9(*a*), (*b*), plate 2). The flow field has

the following general features, which have been numbered and which are discussed in more detail later.

The flow upstream has an oscillatory character made up of two distinct features. Region I is a region of velocity defect, i.e. velocity smaller than free stream, surrounded by region V, which has a velocity in excess of the free stream value. They have been given different numbers because fluid within them behaves in a different fashion as it approaches the sphere. Fluid that starts within the shear layer (region V) is being constantly accelerated and the layer becomes thinner. Close to the sphere the excess velocity has become 25–50 % larger than free stream, the actual magnitude depending on the parameters of the flow. Maximum velocity is reached just beyond the sphere equator. The layer which emerges from behind the sphere (region VII) is narrower than its upstream counterpart, does not spread as rapidly and has a larger angular velocity. In transporting a ring of fluid from a given radius upstream to a smaller radius downstream a larger rotation rate is needed to approximately conserve angular momentum in this almost-inviscid flow. What happens to the fluid in the intermediate region VI is not as clear as it was in the previously reported case (Maxworthy 1968*b*). A vortex jump is still found to occur and its location and intensity determine, or are determined by, the pressure in the rearward slug. By this we mean that the flow and pressure created by the jump must also be compatible with the conditions within the almost-stagnant region, which are themselves the result of the need for compatibility between the slug rotation rate and the Ekman layer flux (Moore & Saffman 1968).

Since vortex-jump phenomena have been observed at several locations within the flow it seems appropriate to consider their characteristics in more detail at this juncture. At the moment the most useful description is due to Benjamin (1962) and (1967). Like the better-known hydraulic jump the vortex jump is considered to be a finite amplitude transition from an initial supercritical flow to a subcritical conjugate flow. Its occurrence in the present instance is so reminiscent of the analogous case of free surface flow (figure 18(*a*), plate 6) that there seems little doubt as to the veracity of Benjamin's concept. Jumps have been found to occur under a variety of circumstances, and since there is no detailed theory useful in all cases the hydraulic analogy is a convenient way of classifying and qualitatively discussing the observed flows.

Unlike fluid from region V, the fluid from region I slowly decelerates as it approaches the sphere. At the tip of the stagnant region (II) it suddenly decelerates, from a finite fraction of U_∞, to essentially zero, within a very short distance. At the same time, its swirl velocity increases rapidly and viscous forces are very important in increasing the slug pressure considerably above free-stream stagnation pressure. Once within the stagnant region, this fluid is slowly drawn into the Ekman layer on the sphere at a rate determined by the slug rotation speed. Once this flow rate has been set, the fluid passes around the equator of the sphere and is ejected from a modified Ekman layer at the rear of the sphere. Since the out-flow is set, by the upstream flow, the rear rotation rate and slug pressure must adjust themselves just to allow the given mass flow to be ejected. Unfortunately, this Ekman layer is not of a simple form and displays

the difficulties described in Maxworthy (1968*b*). Fluid is not smoothly ejected over the whole layer, but tends to form a central jet which goes through a vortex-jump process before it forms the rear slug. The outer shear layer and the slug region are of the same thickness, at the low values of T of these experiments, so that the interaction between the flows in regions III and VI is significant and one is not justified in considering them separately as in Maxworthy (1968*b*). From these qualitative considerations, one can see the numerous interactions which go into deciding the total flow, and we are now in a position to discuss each of the features in detail.

4.2. *Results of flow-field measurements*

Region II is the forward stagnant region or slug. It is probably the most striking feature that one can observe using dye as a fluid tracer. It is a sharply defined region of almost stagnant fluid; that is, the axial velocity is very low, although the relative swirl velocity can be quite large. A slow axial motion is induced by the flow into the Ekman layer required to match the difference between the swirl velocity of the slug and that of the sphere. Far upstream, this small axial flow must come from a streamtube located very close to the axis of symmetry. When a particle reaches the nose of the slug, its axial and swirl velocities are very drastically and rapidly changed (figure 9(*c*), plate 2, and figure 10, plate 3), and the processes which occur are of some significance, as will be shown when detailed velocity measurements are presented. The length of the slug is an obvious feature to measure. It can be done in two ways: using hydrogen bubbles to locate the nose region where the axial and swirl velocities change rapidly, and by using the dye technique described in § 2.3. Because of the slow axial velocity in the slug, and the consequent leakage of dye from the front to the rear of the sphere, the dye column changes length as the sphere rises. By taking pictures at several axial positions of the sphere (figure 8(*a*), (*b*), (*c*), plate 1) and extrapolating the dye column length to the length it has at the sphere's starting position, agreement between the two methods is obtained. Results are shown in figures 11 and 12. For large T, as N increases, the slug length grows exponentially. Even for N as small as 0·5, there is evidence of a very small slug. The rapid collapse of the stagnant region as N is slightly decreased below 4 or 5 is certainly the reason Taylor (1922) missed its existence when N was below his often-quoted value of 2π. The argument given by Greenspan (1968, p. 200), based on the velocity required to maintain the head of a propagating inertial wave stationary with respect to the body, is more realistic for it gives a value of $N \sim 3$ for the location of the transition between short and long slugs.

For most values of T the slug length reaches a maximum or asymptotic length when N is beyond 5. Even though they are not shown, results for $N \sim 100$ give the same lengths as $N \sim 10$, as indicated by comparing figures 8(*b*) and (*d*) (plate 1).

The only deviation occurs for small T, i.e. $O(10)$, for which it was not possible to extend the range of N beyond 10. The asymptotic values are plotted *versus* T on figure 12, where it can be seen that $L/a = T/17$, which is one order of magnitude smaller than the length suggested by the arguments which led to the

qualitative picture shown in figure 1. There are at least two possible reasons for this large discrepancy. One is easy to check, the other is not, at least in the present apparatus. First, the theory does not take account of the effect of the Ekman layer flux on the outer flow. At large T and N, using the apparatus of figure 3(*c*), we can change this boundary-layer flux by changing the rotation rate of the sphere. Ultimately, the rotation rate of sphere and slug could be

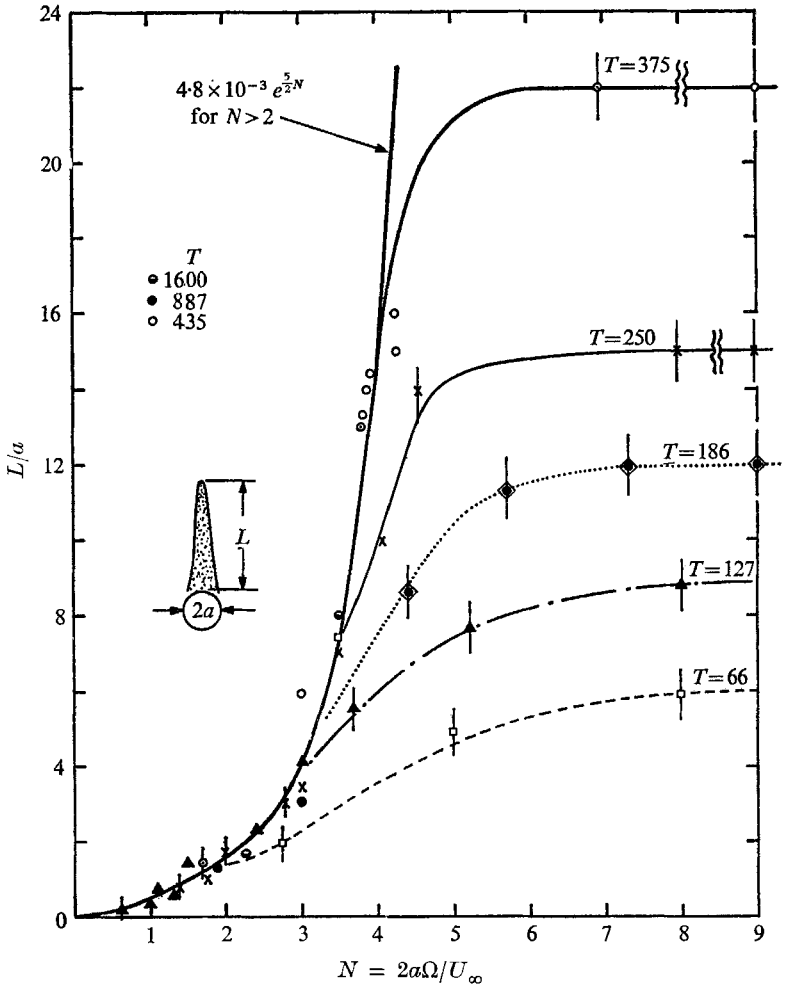

FIGURE 11. Length of the forward stagnant region (L/a) *versus* N for various T.

matched precisely and the flux reduced to zero. Results of such tests, although interesting, do not give the dramatic result that we seek. The slug does not suddenly grow ten times larger when we reduce the boundary-layer flux towards zero. There are subtle changes, small adjustments in length and shape, the appearance of instability, but apparently this mechanism is not the dominant one which, in some sense, sets the scale of the upstream flow. The second possibility concerns inertial effects within the flow. Certainly they have been ignored in the theory,

and on superficial inspection we would seem to have ruled them out experimentally. To the accuracy to which the experiments can be performed, we find that the slug length does not change for N between 5 and 100, for large enough values of T; i.e. *apparently* inertial effects do not affect the important dynamics within the forward disturbance when they are made somewhat smaller than the Coriolis forces. The question becomes: is an N of 100 large enough? Related

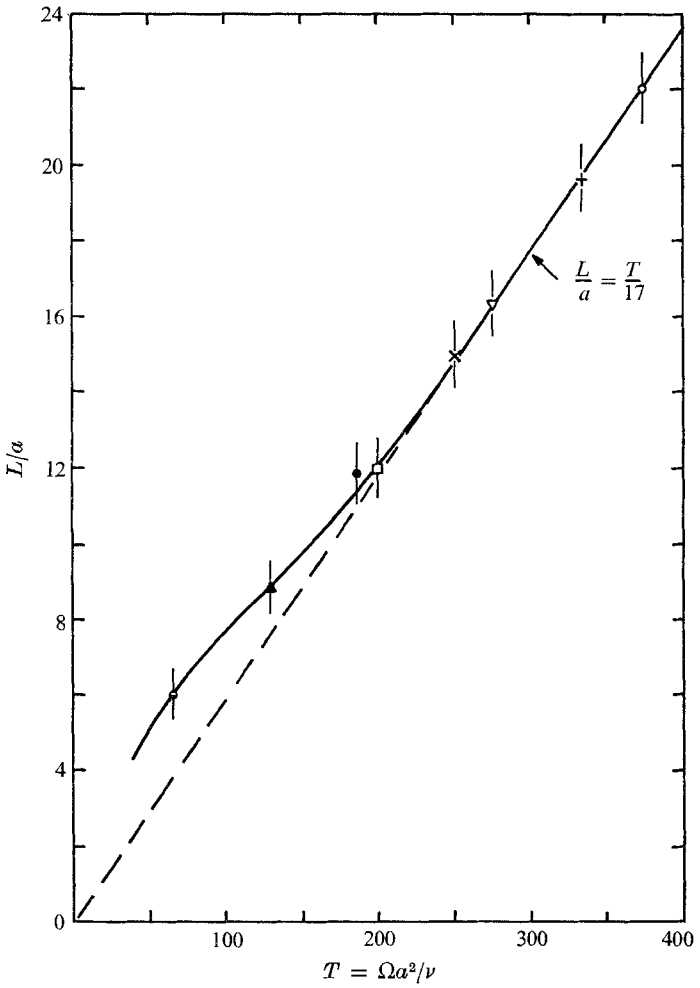

FIGURE 12. Asymptotic value of L/a *versus* T for large values of N.

work designed to determine the effect of end walls on these flows (Maxworthy 1968*b*) and for which there is also an exact linearized solution (Moore & Saffman 1968) strongly suggests that in the present case we are far from the slow-flow limit. In that work, the appropriate magnitudes were found to be that R^2/N should be at least $O(10^{-9})$. Or that inertia forces should be very much smaller than *both* Coriolis *and* viscous forces. Typically this parameter has a value of unity in the experiments being reported! For the values of T of these experiments

N would have to be $O(10^6)$ for R^2/N to be of the magnitude stated. Of course, this argument requires that the same parameter be the correct one for the present case. It seems very unlikely that it will, but at least it points to the possibility of inertial effects still being important, and eases the dilemma of having a perfectly acceptable theoretical solution but being unable to approach it in an experiment which was originally designed, in part, to do so.

The hydrogen-bubble technique can give further information about this region and is especially useful in deciding the slug structure when $N > 6$; that is, large enough for the slug to have reached its asymptotic length (figure 13, plate 4). The technique described in § 2.3 and shown on figure 4 was used to determine the axial and azimuthal velocity profiles. Since most of the terms in the radial momentum equation are small compared to the Coriolis term we can reconstruct the pressure gradient and hence the pressure ($\tilde{p}$) from a modified geostrophic equation,

$$\frac{1}{\rho}\frac{\partial \tilde{p}}{\partial \tilde{r}} = 2\Omega \tilde{v}_\theta + \frac{\tilde{v}_\theta^2}{\tilde{r}} \tag{1}$$

and the boundary condition that $\tilde{p}$ equals $\tilde{p}_\infty$† at large $\tilde{r}$. Whence

$$\tilde{p} - \tilde{p}_\infty = 2\rho\Omega \int_\infty^{\tilde{r}} \tilde{\omega}\tilde{r}\, d\tilde{r} + \rho \int_\infty^{\tilde{r}} \tilde{\omega}^2 \tilde{r}\, d\tilde{r}, \tag{2}$$

$\tilde{\omega}$ being the local angular velocity as found from the construction of figure 4.

In dimensionless form this becomes,

$$C_p - C_{p_\infty} = 2N^2 \left[2 \int_\infty^r \omega r\, dr + \int_\infty^r \omega^2 r\, dr \right], \tag{3}$$

where $\tilde{p}$ has been made dimensionless in units of $\rho U_\infty^2/2$, $\tilde{\omega}$ in units of Ω and $\tilde{r}$ in units of a.

Results of such a measurement are shown in figure 4, where typical velocity and pressure profiles are plotted for a downstream wake.‡ Figure 15 shows how the pressure on the centre line, and within the slug, varies with N. The pressure is much larger than free-stream stagnation pressure, and we must now decide on a consistent mechanism for the formation of such a large pressure.

Up to this point, we have treated the upstream slug as an isolated phenomenon when it is, in fact, surrounded by other features (regions I and V) which are important in themselves and lead to the required new insights into the structure of the slug. These regions comprise the flow upstream of the slug (regions I) and a region of accelerated flow (region V) immediately surrounding the slug.

In region I the axial velocity is everywhere markedly non-zero. Disturbances decay as we move upstream, i.e. uniform flow conditions are approached, until the flow merges into the appropriate, limiting Oseen flow, as discussed by Childress (1964) or into the appropriate inviscid flow, as discussed by Miles

† The subscript ∞ refers to conditions in the undisturbed flow far upstream.

‡ This method is less useful when the slug length is short, since axial flow gradients become important and invalidate the assumptions basic to the method. It is at best of qualitative use under these circumstances. The values plotted in figure 15 are for long slugs for which (1) is valid.

(1969*a*, *b*). The swirl velocity is small everywhere, so that when we observe the flow, using the hydrogen-bubble technique, a good representation of the axial velocity profile is obtained without having to resort to further data reductions. Figure 14 (plate 5) and figure 10 (plate 3) are typical photographs. Several interesting observations emerge. We may compare these results to theoretical predictions of Stewartson (1958) and Miles (1969*a*). Direct comparison with the results for a sphere yields no agreement for the upstream flow. However, if we

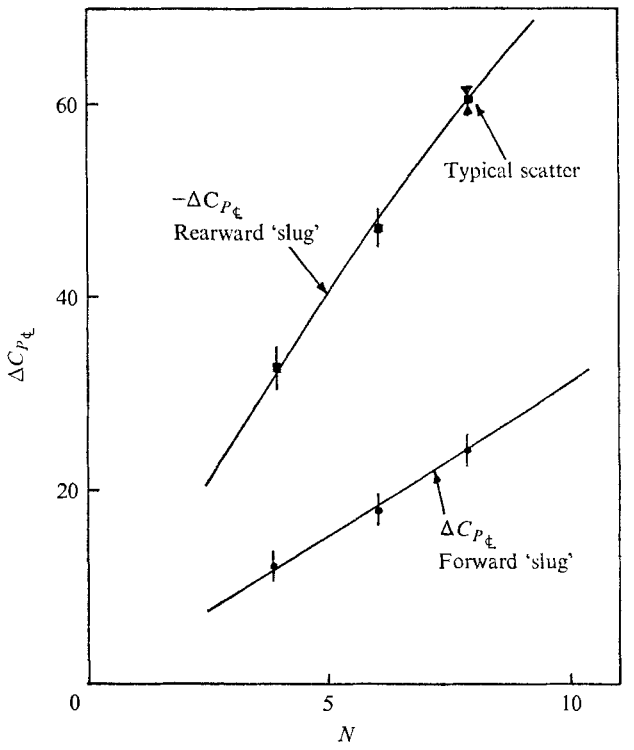

FIGURE 15. Variation of stagnant region centre-line pressure with N and T for various axial locations. Upstream and downstream slugs.

assume that an inviscid outer flow is passing over a composite body made up of the sphere plus the forward stagnant region, startling agreement with the inviscid slender ellipsoid theory of Miles (1969*a*) is obtained.† Figure 16 shows these comparisons for the centre-line velocity for values of N and T, for which the stagnant region is not too long, and for which velocity profiles at several axial locations are available. Whether such conclusions are valid for larger values of N and T, i.e. for long slugs, is not known because of the limited axial extent of the experiments. Further support for the point of view in Miles (1969*b*) comes from observing many photographs like those shown in figure 15 (plate 5) and figure 10 (plate 3). Invariably at low values of N the velocity profiles closest to the body

† The author is indebted to J. W. Miles for suggesting this method of comparison, which is also reported, in numerical form, in Miles (1969*a*). It is also implicitly assumed that the rearward flow has a small effect on the flow upstream.

consist of a series of oscillations, rather like the zero-order Bessel function, which change, as we go farther from the body, to profiles with fewer and fewer obvious wiggles. Unfortunately the data is not precise enough to compare, with any great confidence, to the theory and we are left only with the quantitative data of figure 16 and the qualitative observations shown in the plates. This upstream flow is matched to the conditions in the slug through a vortex-jump region

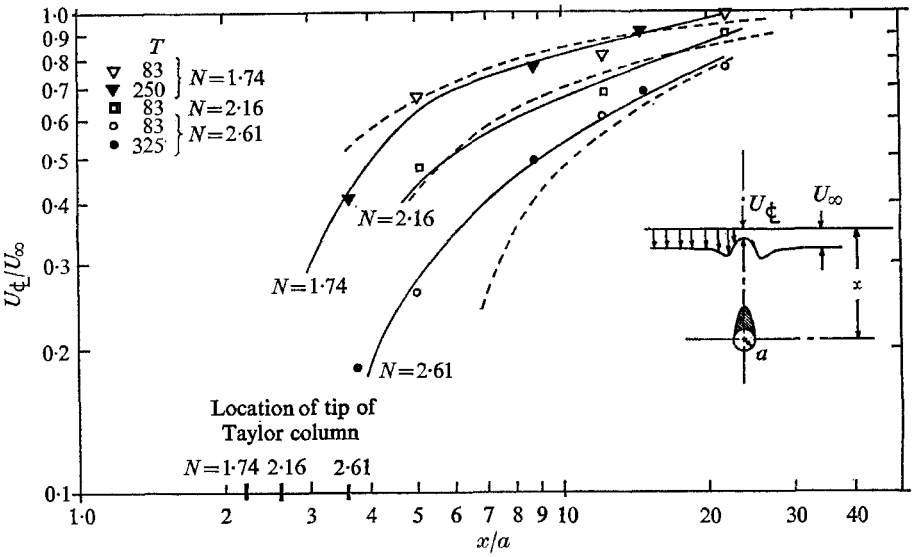

FIGURE 16. Centre-line velocity ahead of the upstream stagnant region for various values of T and N. Theoretical results of Miles (1969) for an ellipsoid with the same fineness ratio as the composite body made up of sphere-plus stagnant zone. ——, present experiment; – – –, theory.

within which the axial and swirl velocities are very rapidly changed. In figure 9(*c*) (plate 2) and figure 10 (plate 3) we see the very rapid deceleration of the flow that takes place. Plotting the axial centre-line velocity in figure 17 shows that the velocity is reduced from a large value to essentially zero within a length of the order of the body radius. At the same time, the swirl velocity changes rapidly from small values to large values, indicating, through (2), a large axial pressure gradient.

Such an observation now allows us to tie several of our previous results together, in particular the short forward slug length and the high slug pressure are consistently explained. Along the centre-line, only viscous forces can elevate the pressure above the free stream stagnation pressure (p^0_∞), i.e.

$$\frac{\partial}{\partial x}p^0 = \frac{\partial}{\partial x}[p + \tfrac{1}{2}v_x^2] = \frac{1}{R}\left[\frac{\partial^2 v_x}{\partial r^2} + \frac{\partial^2 v_x}{\partial x^2}\right], \dagger \tag{4}$$

if it is assumed that initially the viscous forces due to gradients in both r and x directions are equally important. If l and δ are typical length scales in the x

† Quantities have been made dimensionless with respect to the free stream velocity (U_∞), dynamic pressure ($\frac{1}{2}\rho U_\infty^2$) and body radius ($a$).

and r directions, respectively, then the change in p^0, with v_x of order unity, is given by

$$\Delta p^0 \sim \frac{1}{R}\left[\frac{l}{\delta^2}+\frac{1}{l}\right]. \tag{5}$$

Most observations bear out the fact that $l > \delta$, whence $\Delta p^0 \sim l/R\delta^2$.

In the theoretical work on this problem, the adjustment to $\Delta p^0 \sim O(N)$ takes place with $\delta \sim O(1)$ and $l \sim O(T)$. In the present experimental work the adjustment probably takes place with $l \sim O(1)$ and $\delta \sim O(T^{-\frac{1}{2}})$ under most circumstances. However, as viscous effects become more important, at large T and

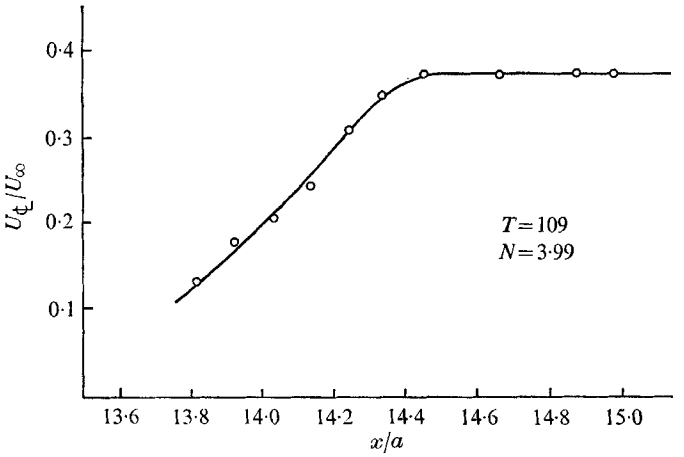

FIGURE 17. Centre-line axial velocity *versus* axial location, showing the rapid deceleration of flow at nose of the stagnant region for $N = 3{\cdot}99$, $T = 435$.

small R, the region becomes more smeared out and some statement intermediate between these two becomes appropriate. The observation that the flow adjusts itself so that the static pressure changes in a short axial distance is important and qualitatively bears out the numerical calculations of Bossell (1967), in which it is decided that this rapid transition is, in fact, a vortex jump in the rotating flow. This again shows that for our relatively large $R[\sim O(10)]$ and large $N[\sim O(10^2)]$ inertia forces are still important, since they must be considered in such a rapid transition. The need to perform experiments at smaller values of R and larger values of N is obvious, but only by major modification of the present apparatus could such measurements be made.

Similar arguments, based on viscous effects, also hold downstream, where the pressure must change from being negative and $O(N)$ (see figure 15) to the static pressure at infinity. Unlike the forward slug, however, no regions of rapid axial change have ever been noted in the downstream flow, and the adjustment is always made in an extensive axial distance, presumably of order T long.

The central slug region II has a natural extension around the sphere and into the central region behind the sphere (regions III and IV). Fluid from II is sucked uniformly into the Ekman layer on the sphere, it flows around the sphere equator in a thin high velocity sheet and is then ejected into the rearward, low

axial-velocity slug. The character of the ejection process is interesting and is unlike the process that one might expect from such an Ekman Layer. The reader is referred to Maxworthy (1968*b*) for a discussion of this process when T is very large; for the present relatively small values of T the details are somewhat different. Boundary-layer fluid instead of being smoothly ejected tends to form a concentrated rapidly swirling jet at the lower pole of the sphere. This jet then rapidly spreads to a larger radius with lower axial and azimuthal velocities. Figure 9(*a*) (plate 2) shows this in a very convincing manner when N is small and consequently the velocities within the slug regions are not small. Such evidence points to the bursting being yet another form of vortex jump or breakdown, first found within the vortices above delta wings at angle of attack, but subsequently observed in many types of rotating-flow experiment. As N increases in magnitude and the axial velocities within the slugs become smaller, the jump becomes of smaller and smaller axial extent until it has the oscillatory form shown in region III of figure 7. At this stage, dye observations show that the central part of the downstream slug is filled with clear fluid surrounded by an annular dye column (as drawn in region IV of figure 7). This again is characteristic of strong vortex-jump conditions, partially explained in Benjamin (1962) and also found in strong concentrated vortices (Maxworthy 1967). As N is increased further, it becomes more difficult to observe the details although one can say, without hesitation, that something out of the ordinary is happening in this region. Again, the hydrogen-bubble method gives details of the velocities in region IV as shown in figures 4 and 18(*b*) (plate 6). The pressures can also be calculated, as for the forward slug, and are plotted in figure 15. The angular velocities are larger in magnitude than those in the forward slug, so that the magnitude of the lower pressure in the rear slug is larger than that of the elevated pressure in the forward slug. The increased drag of the sphere comes more from the decreased rearward than from the increased upstream pressure.

By concentrating our attention on particles which are close to the centre-line, we have so far missed the interesting details of the flow at larger radii (regions V, VI and VII), where there exists a velocity in excess of the free-stream value. This accelerated region has two reasons for existence, one being associated with the inviscid or wave drag, and the other with the viscous wakes and form drag. In inviscid flow, the wave drag appears as a large decrease in pressure over the rear of the body. The only way to get a large suction, if p^0 is to remain constant, is for there to be a large excess velocity over the rear of the sphere; cf. stratified flow and free surface flow over an obstacle (figure 18, plate 6). This region is fed from upstream between two stream surfaces that come closer and closer together as the body is approached. A locally supercritical flow is formed, which jumps at some location to a subcritical state. For the free surface case we have a hydraulic jump, and in the rotating case a vortex jump. Secondly, the viscous wakes act as sources and sinks of fluid, in an unsteady flow (figure 19). The effect of rotation is to channel this fluid motion into a narrow annulus surrounding the almost stagnant region. Unfortunately, the method of measuring the swirl velocity and inferring the pressure field is not very sensitive in these regions because of the very small magnitudes of the velocities. However, oblique views of sheets of hydrogen

bubbles and even imaginative interpretation of pictures such as figure 9(*c*) (plate 2), figure 10 (plate 3) and figure 18(*b*) (plate 6) show that flow in this region is rotating slowly in a positive direction.† From (2), this means that the pressure is below the static value at large distances. Whether this just indicates that the flow along these stream lines is essentially inviscid, so that p^0 remains

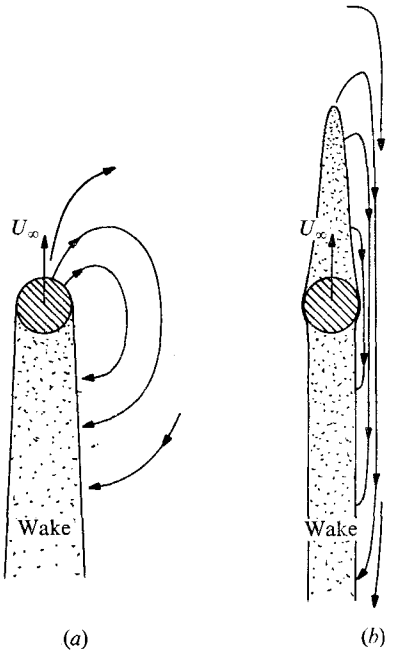

FIGURE 19. Physical explanation for region of high velocity surrounding stagnant slug. Upstream slug acts as a source and downstream slug as a sink of fluid which is channelled by the constraint of rotation into a narrow annular region.

constant, or whether p^0 has been decreased by viscous action, cannot be stated with certainty at this point. A crude estimate based on oblique views would suggest that the former possibility is closely realized, but the evidence is not conclusive.

4.3. *Comments on the interaction between the various regions of the flow field*

Now that the details of the flow field have been presented it is useful to try to fit them into a consistent physical picture. The easiest case seems to occur when N is less than about 5 or 6. In this case the nose of the upstream Taylor column always appears abruptly, and the inviscid theory of Miles (1969*a*, *b*) seems to describe the flow development ahead of the body and slug. Then the flow upstream of the sphere must consist of the following closed system of interactions, all of which are interdependent. The inviscid flow upstream of the slug is supercritical by Benjamin's (1962) criterion and becomes closer and closer to critical as the tip of the slug is approached. A vortex jump occurs at a value of the

† The basic rotation has a positive direction, as does swirl in the rear slug. Swirl in the forward slug has negative rotation.

Benjamin number† for which a matching to the subcritical interior slug flow can be made. This subcritical flow is in turn controlled by the need to satisfy the downstream conditions at the surface of the sphere; that is, with flow into the Ekman layer, and presumably some inertial radial flow, setting the mass flow and the slug rotation rate. The length and shape of the slug so formed in turn determines the nature of the upstream inviscid flow that started the discussion. This series of interactions (inviscid flow–vortex jump–subcritical slug–flow over sphere–inviscid flow) immediately suggests the form of the analogous free surface flow. The initially supercritical flow is modified by bottom friction in this case. A hydraulic jump occurs in front of an obstacle at a location where the supercritical flow has lost enough momentum to match the downstream conditions. The latter are in turn set by the flow over the obstacle itself. In this case it is obvious that the upstream influence of the body only reaches as far as the jump region, the supercritical flow upstream being unaffected by the body's presence. In the rotating flow case the statement cannot be as strong, since the upstream, supercritical, inviscid flow is affected by the shape of the slug–sphere combination. However, wave propagation from the body can only be felt as far as the location of the vortex jump and flow ahead is free of waves moving upstream.

Flow downstream of the sphere is complicated but seems free of any controversy. Boundary-layer fluid being ejected from the rear Ekman layer forms a swirling jet which breaks down to form the rearward, subcritical Taylor column. The slug pressure and rotation so formed must also match that created by the vortex jump of the high-velocity annular jet which comes from the upstream inviscid flow.

What happens when N becomes large is less clear. The downstream flow is qualitatively the same but the upstream flow is changed. The vortex jump region becomes smeared out and viscosity acts over a larger axial distance. It seems incorrect to talk of an outer inviscid flow in this case and perhaps the matching takes place either directly, or through another buffer region, to the far field solution of Childress (1964). Because of their limited axial extent the present experiments can make no definitive statement about this case.

4.4. *Similarities to the flow of a stratified fluid over an obstacle*

Similarities to the case of a continuously stratified fluid flowing over an obstacle should be brought forth at this point. Several investigations have appeared recently : Miles (1968*a*, *b*) on the flow of an inviscid stratified fluid, and Martin & Long (1968), Janowitz (1968) and Pao (1968) on flows with modifying effects of viscosity alone included or viscosity and fluid inertia included. Again the problem arises: under what circumstances is an inviscid solution a valid approximation to the flow ahead of the body and at what point must viscosity be included. As we have already seen, an identical question arises in the present rotating-flow case. The strongest statement that one can make is included in § 4.3 and suggests that the inviscid solution is valuable under some circumstances. How this statement can be extended into the stratified flow problem is not clear at the moment,

† The Benjamin number is the swirling flow equivalent of the Froude number of free surface flows. See Benjamin (1962, p. 601), for a precise definition.

mainly because of our ignorance of the details of upstream slug formation in this case. To the author's knowledge, nobody has observed an internal hydraulic jump at the nose of the blocked region so that viscosity may well be a more important effect in this case. To carry the similarity between the two cases still farther, the above-mentioned studies all show jet-like regions in the far field in which the velocities are alternately larger and smaller than the free stream value as transverse distance increases. The present results show the same effects (see e.g. figures 9 (*c*), plate 2; 10, plate 3; 13, plate 4; 14, plate 5). Although as N and T increase, the outermost jets become weaker and weaker until only one accelerated region (region V, figure 7) can be clearly seen.

5. Transient flow observations

From the results of § 3 and experience gained in observing large spheres rise through short cylinders, it is apparent that a weak interaction is taking place between the wakes created by the motion and the end wall of the apparatus. That it is a small effect in the present case is obvious from the magnitude of the correction applied and the fact that no effects attributable to variations of sphere diameter were found in the present experiments. In order to investigate the matter further, a series of transient experiments were performed, all of which pointed to the small effects of end walls on the results. The rationale and methods were as follows:

(i) If the free sphere was released from the apparatus of figure 3 (*b*), and reached its terminal velocity before dye observations showed waves propagating from the body hitting the end wall, then the end-wall effects could be considered small.

(ii) If the towed sphere was started impulsively from rest in the apparatus of figure 3 (*d*) and the hydrogen-bubble pictures indicated that the flow field in the neighbourhood of the sphere had reached a steady state before waves from the body had had time to reach the end walls, then end-wall effects could be considered small. It is apparent from the manner of problem statement that negative results were found in both cases.

As a bonus from these latter measurements, it is possible to determine the velocity with which disturbances propagate away from the body along the axis of rotation. From the photographs it was determined that the velocity, in one case, was $3{\cdot}0 \pm 0{\cdot}1$ cm/sec, equivalent to the velocity of an inertial wave of wavelength $2{\cdot}36 \pm 0{\cdot}05a$. The calculation performed by Greenspan (1968, p. 200) gives a wavelength of $2{\cdot}12a$. The head of the propagating wave was very similar in nature to the head of the steady Taylor column, i.e. the axial velocity was brought to zero, and the swirl velocity increased within a short axial distance.

It is apparent from these discussions that the nature of the wall interaction is similar to that described by Moore & Saffman (1968) and that the flow in the wakes is slightly affected by the need to satisfy the boundary conditions appropriate to a divergent Ekman layer at the end walls.

6. Conclusions

Measurements of the drag coefficient (C_D) of a sphere rising through a rotating cylinder of water have produced the following results. (*a*) For small values of N, C_D is less than the value for $N = 0$; (*b*) for large T and N,

$$C_D = (2{\cdot}60 \pm 0{\cdot}05)\, N^{1{\cdot}00 \pm 0{\cdot}01};$$

(*c*) for large T and $1{\cdot}4 < N < 4$,

$$C_D = 4{\cdot}10 \pm 0{\cdot}10 N^{2{\cdot}00 \pm 0{\cdot}02}.$$

Flow field observations using various dye and hydrogen-bubble techniques show the following features. (*a*) Stagnant regions are formed up- and downstream of the sphere. Within the upstream slug is a positive static pressure of $O(N)$ and a slow axial flow that feeds an Ekman layer on the sphere surface. This fluid flows around the sphere equator and is ejected as a jet, followed by a vortex jump, into the downstream slug. Pressure in this slug is negative and $O(N)$. (*b*) Surrounding these slugs is an annular region with a velocity larger than the free-stream value. Flow approaching the sphere from upstream accelerates, forms a vortex jump beyond the equator and then decelerates slowly downstream under the action of viscosity. (*c*) The upstream slug has length (L) which is given by: $L/a = T/17$ for $N > 6$. Flow approaching the tip of this slug is decelerated within a small axial distance, defining the beginning of the slug very accurately. Because the flow downstream changes so slowly, it is not possible to make a similar measurement there.

Duncan E. Griffith designed and constructed most of the apparatus, and to him should go the praise for any success this work might have.

Much of the work reported here was performed at the Jet Propulsion Laboratory, Pasadena, California, and supported by the National Aeronautics and Space Administration, contract NAS7-100. It was completed under the sponsorship of the National Science Foundation, grant no. GK 2731 to the University of Southern California, Department of Aerospace Engineering, Los Angeles, California.

REFERENCES

Benjamin, T. B. 1962 Theory of the vortex breakdown phenomenon. *J. Fluid Mech.* **14**, 593.

Benjamin, T. B. 1967 Some developments in the theory of vortex breakdown. *J. Fluid* Mech. **28**, 65.

Bossel, H. H. K. 1967 Inviscid and viscous models of the vortex breakdown phenomenon. Report no. AS-67-A, College of Engineering, University of California, Berkeley.

Bretherton, F. P. 1967 The time dependent motion due to a cylinder moving in an unbounded rotating or stratified fluid. *J. Fluid Mech.* **28**, 545.

Childress, W. S. 1962 Rotating, viscous flow past an axially symmetric solid. *Jet Prop. Lab. Space Prog. Sum.* no. 37–18, IV, 46–48.

Childress, W. S. 1964 The slow motion of a sphere in a rotating, viscous fluid. *J. Fluid Mech.* **20**, 305

Grace, S. F. 1926 On the motion of a sphere in a rotating liquid. *Proc. Roy. Soc. Lond.* A **113**, 46.

GREENSPAN, H. P. 1968 *The Theory of Rotating Fluids*. Cambridge University Press.

JANOWITZ, G. S. 1968 On wakes in stratified fluids. *J. Fluid Mech.* **33**, 417.

KÜCHEMANN, D. 1965 Report on the I.U.T.A.M. symposium on concentrated vortex motions in fluids. *J. Fluid Mech.* **21**, 1.

LONG, R. R. 1953 Steady motion around a symmetrical obstacle moving along the axis of a rotating fluid. *J. Met.* **10**, 197.

MARTIN, S. & LONG, R. R. 1968 The slow motion of a flat plate in a viscous, stratified fluid. *J. Fluid Mech.* **31**, 669.

MAXWORTHY, T. 1965 An experimental determination of the slow motion of a sphere in a rotating, viscous fluid. *J. Fluid Mech.* **23**, 373.

MAXWORTHY, T. 1967 The flow creating a concentration of vorticity over a stationary plate. *Jet Prop. Lab. Space Prog. Sum.* no. 37–44, IV, 243–249.

MAXWORTHY, T. 1968*a* Experimental studies in magneto-fluid dynamics: pressure distribution measurements around a sphere. *J. Fluid Mech.* **31**, 801.

MAXWORTHY, T. 1968*b* The observed motion of a sphere through a short, rotating cylinder of fluid. *J. Fluid Mech.* **31**, 643.

MILES, J. W. 1968*a* Lee waves in a stratified flow. Part I. Thin barrier. *J. Fluid. Mech.* **32**, 549.

MILES, J. W. 1968*b* Lee waves in a stratified flow. Part II. Semi-circular obstacle. *J. Fluid Mech.* **33**, 803.

MILES, J. W. 1969*a* The lee-wave régime for a slender body in a rotating fluid. *J. Fluid Mech.* **36**, 265.

MILES, J. W. 1969*b* Axisymmetric flow of a rotating, viscous liquid over a given stream surface. *J. Fluid Mech.* (To be published.)

MOORE, D. W. & SAFFMAN, P. G. 1968 The rise of a body through a rotating fluid in a container of finite length. *J. Fluid Mech.* **31**, 635.

MOORE, D. W. & SAFFMAN, P. G. 1969 The structure of free vertical shear layers in a rotating fluid and the motion produced by a slowly rising body. *Trans. Roy. Soc. Lond.* A **264**, 597.

MORRISON, J. W. & MORGAN, G. W. 1956 The slow motion of a disk along the axis of viscous, rotating liquid. Report 56207/8, Div. of Appl. Math. Brown University.

PAO, H. H. 1968 Laminar flow of a stably stratified fluid past a flat plate. *J. Fluid Mech.* **34**, 795.

PROUDMAN, J. 1916 On the motion of solids in a liquid possessing vorticity. *Proc. Roy. Soc. Lond.* A **92**, 408.

ROTT, N. & LEWELLEN, W. S. 1966 Boundary layers in rotating flows. In *Progress in Aeronautical Sciences*, vol. 7. Oxford: Pergamon.

SCHRAUB, F. A., KLINE, S. J., HENRY, H., RUNSTADLER, P. W. & PITTELL, A. 1965 *Trans. A.S.M.E.* Ser. D, **87**, 429.

SQUIRE, H. B. 1956 Rotating fluids. In *Surveys in Mechanics* (ed. G. K. Batchelor & R. M. Davies). Cambridge University Press.

STEWARTSON, K. 1952 On the slow motion of a sphere along the axis of a rotating fluid. *Proc. Camb. Phil. Soc.* **48**, 168.

STEWARTSON, K. 1958 On the motion of a sphere along the axis of a rotating fluid. *Quart. J. Mech. Appl. Math.* **11**, **39**.

STEWARTSON, K. 1968 On inviscid flow of a rotating fluid past an axially-symmetric body using Oseen's equations. *Quart. J. Mech. Appl. Math.* **21**, 353.

TAYLOR, G. I. 1917 Motion of solids in fluids when the flow is not irrotational. *Proc. Roy. Soc. Lond.* A **93**, 99.

TAYLOR, G. I. 1922 The motion of a sphere in a rotating liquid. *Proc. Roy. Soc. Lond.* A **102**, 180.

TAYLOR, G. I. 1923 Experiments on the motion of solid bodies in rotating fluids. *Proc. Roy. Soc. Lond.* A **104**, 213.

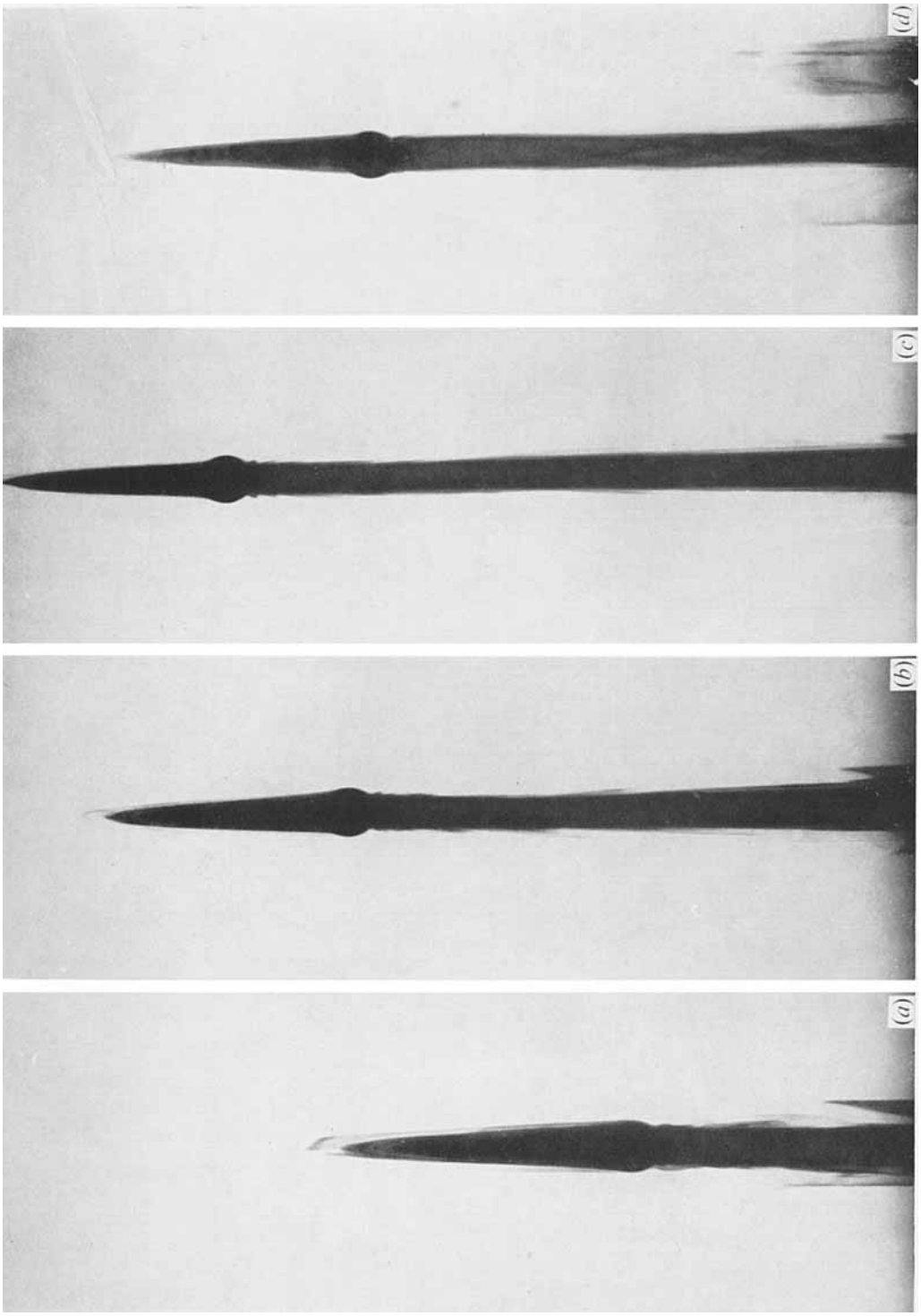

FIGURE 8(*a–c*). Consecutive photographs of a sphere rising from a region of dye concentration. $N = 7{\cdot}38$, $T = 186$. Showing the almost stagnant forward region. (*d*) A photograph corresponding in axial location to (*b*), but with $N = 30{\cdot}6$, $T = 186$.

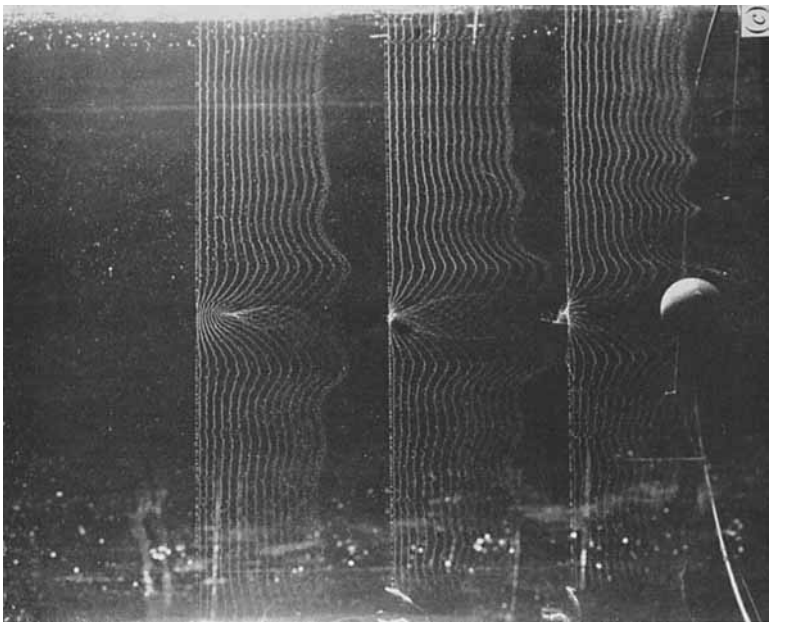

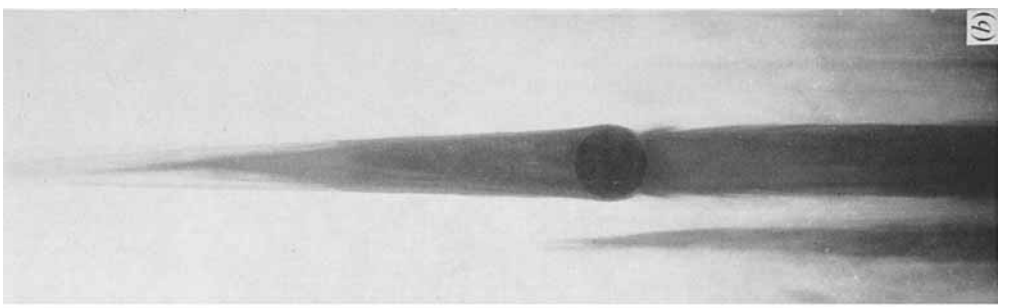

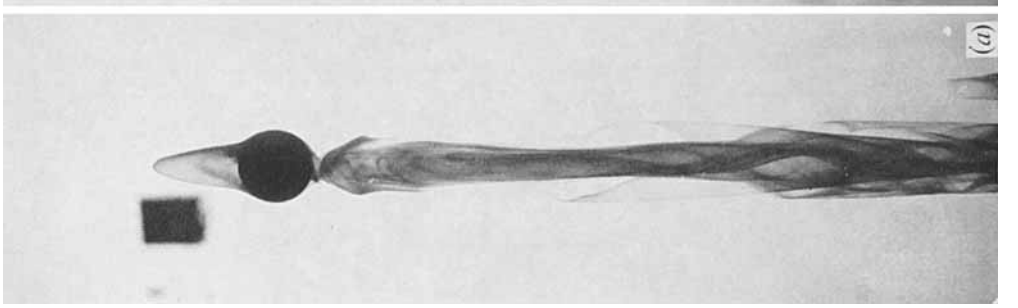

FIGURE 9 (*a*, *b*). Photographs of a sphere rising from a region of dye concentration. For (*a*) $N = 3{\cdot}4$, $T = 152$, showing the nature of the boundary-layer eruption to form the rear wake; (*b*) $N = 35$, $T = 275$, showing the almost conical shape of the forward slug and the behaviour of the boundary layer as it moves around the sphere equator. (*c*) $N = 3{\cdot}99$, $T = 435$, hydrogen bubble picture of the forward wake, using a series of pulses spaced equally in time. Note the rapid decrease in axial velocity of the nose of the slug (upper wire) and the distortion of bubble lines by both rotational and axial motion.

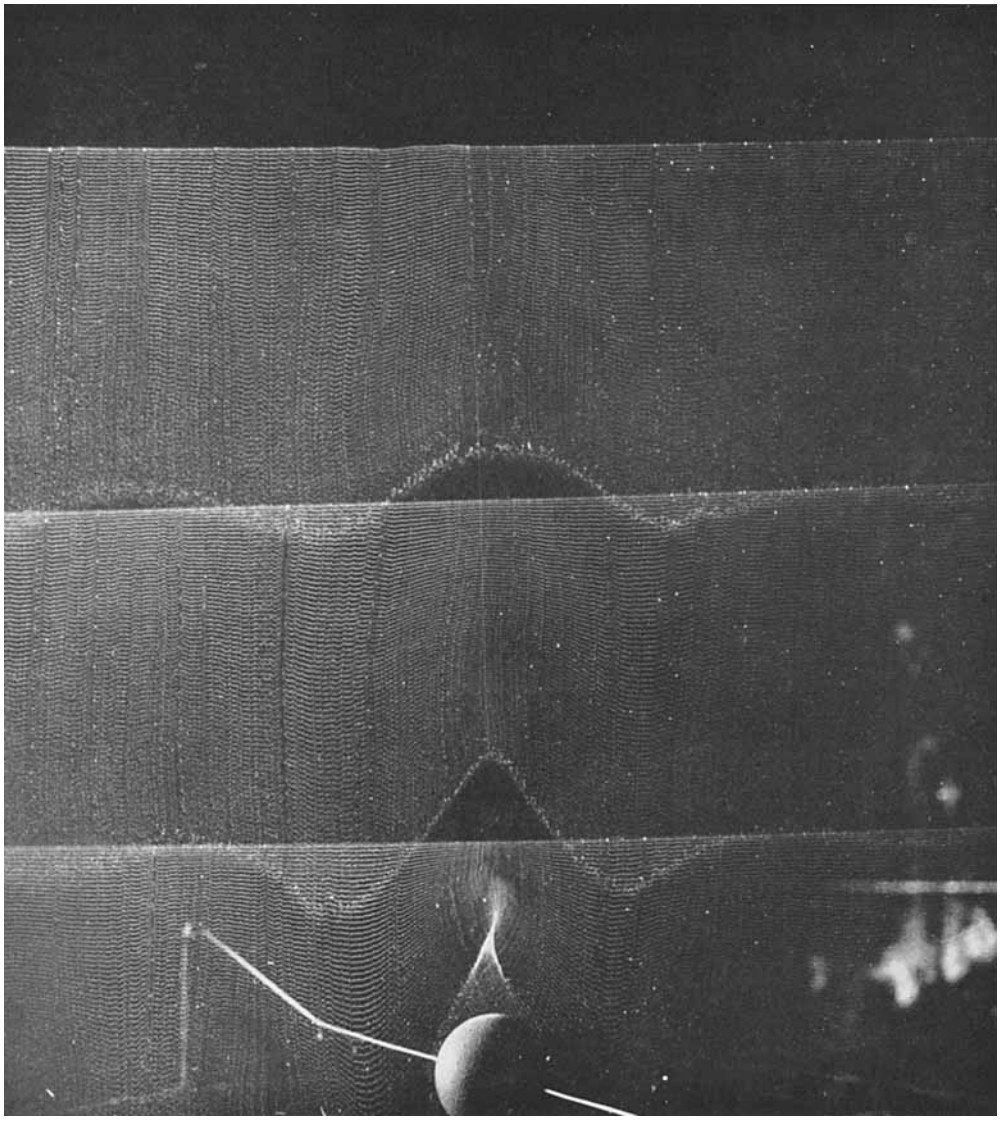

FIGURE 10. Multiple-pulse hydrogen-bubble picture of flow ahead of a sphere for $N = 1{\cdot}75$, $T = 375$. Note the clear definition of the small forward stagnant region for this small value of N.

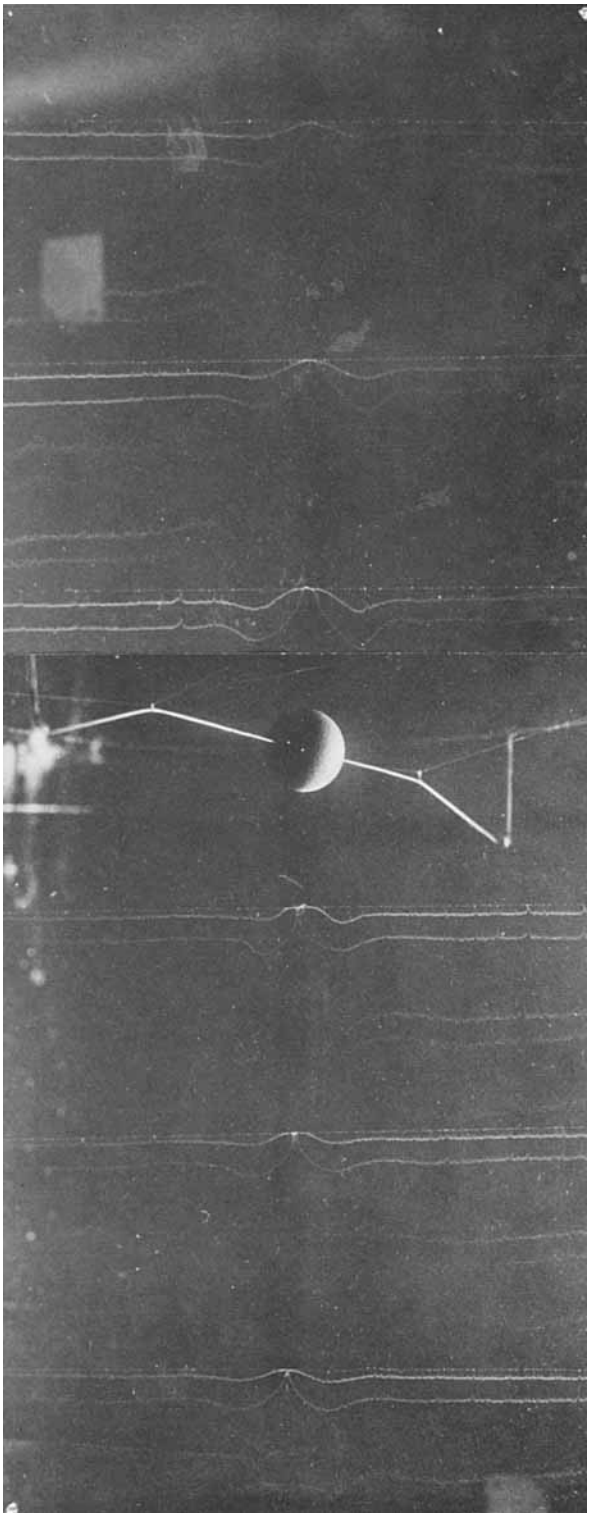

FIGURE 13. A composite hydrogen-bubble picture showing both the forward and rearward slugs for $N = 7{\cdot}93$, $T = 386$. Note the velocity larger than free stream outside the slug region and the slow decay of disturbances both up- and downstream. The shape of the first bubble line formed shows, dramatically, the distortion of this line by the rapid rotation within the slug.

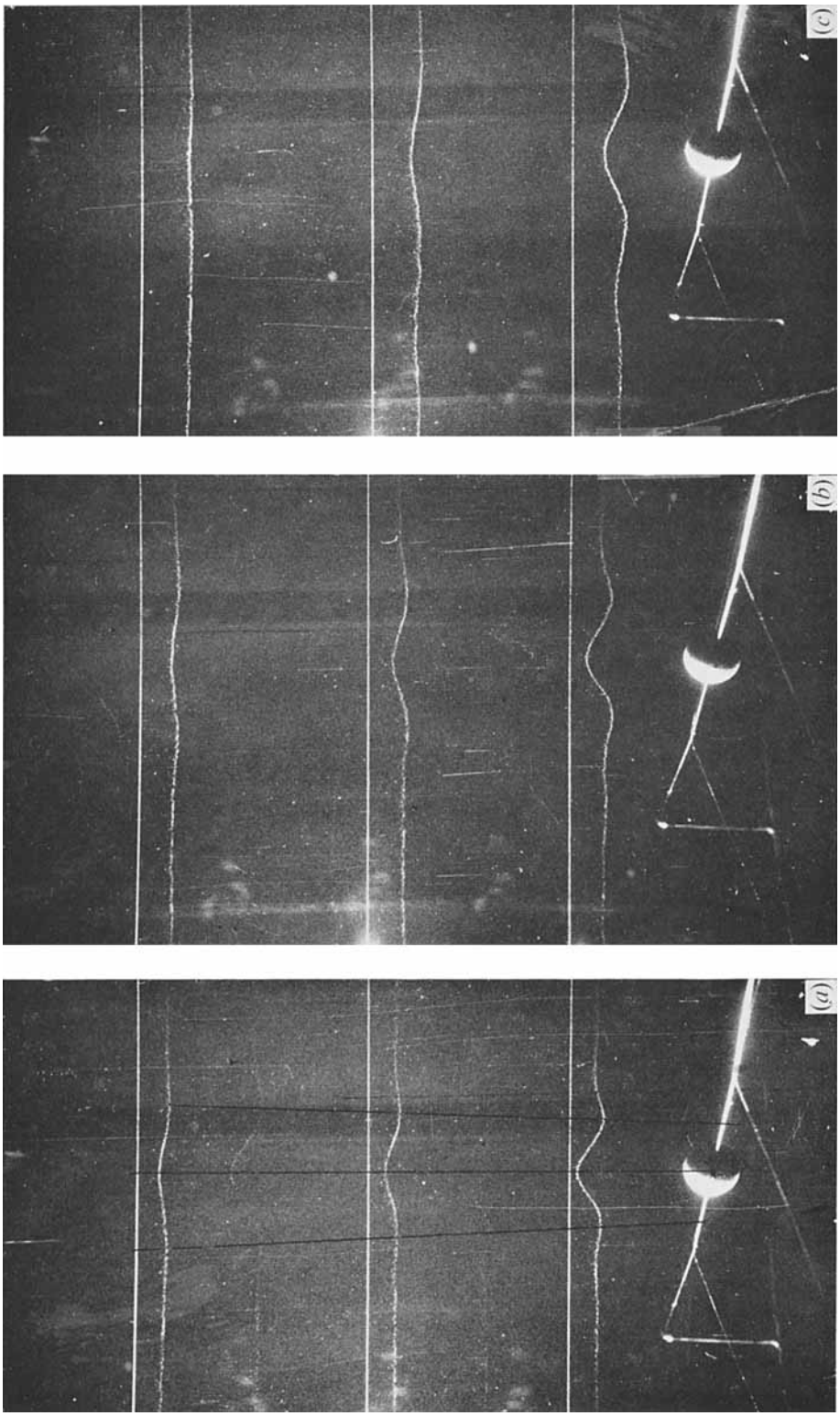

FIGURE 14. Axial velocity profiles upstream of short stagnant regions for the following conditions: (*a*) $T = 83{\cdot}0$, $N = 2{\cdot}61$; (*b*) $T = 83{\cdot}0$, $N = 2{\cdot}16$; (*c*) $T = 83{\cdot}0$, $N = 1{\cdot}74$.

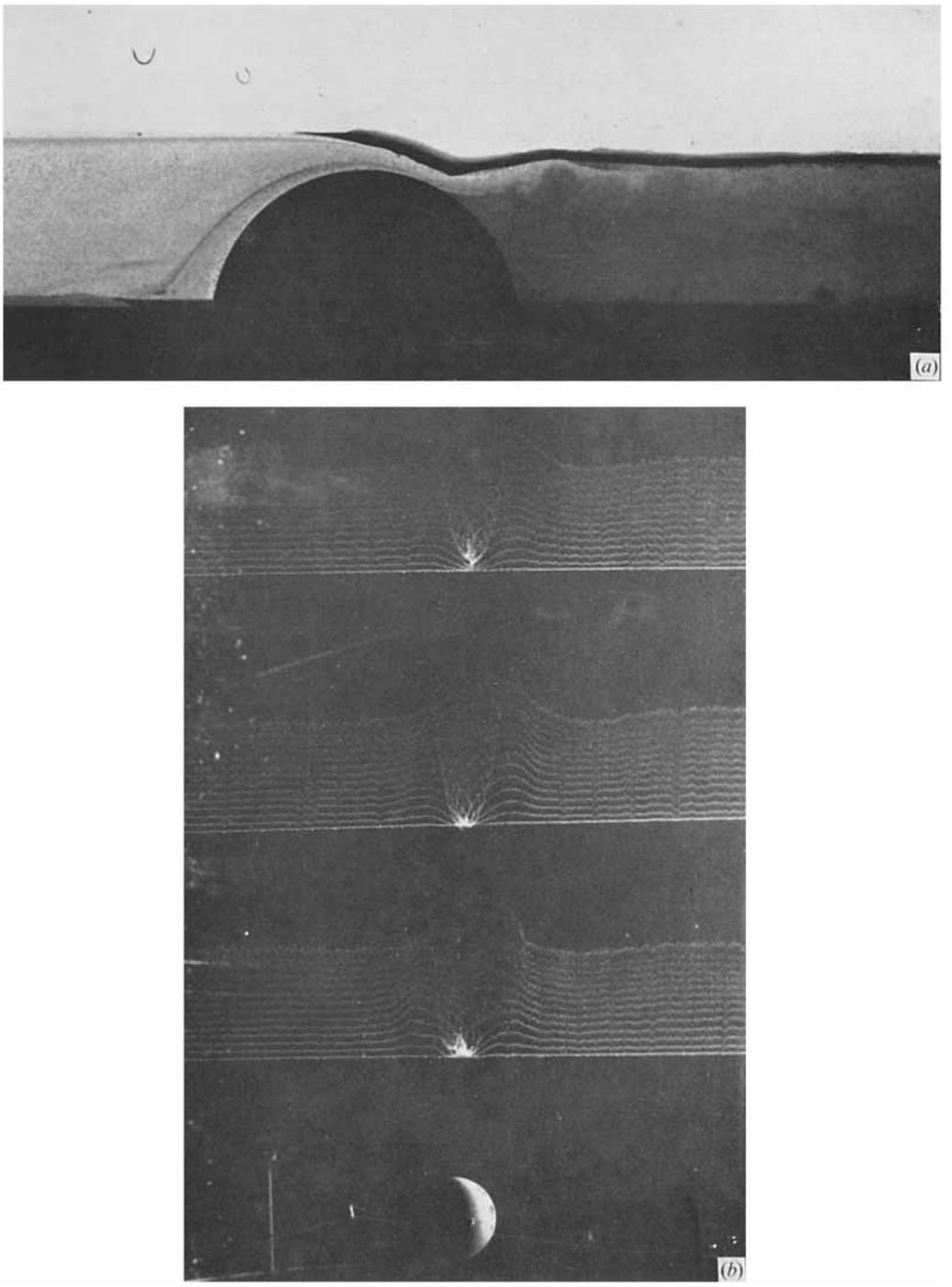

FIGURE 18. (*a*) Free surface flow over an obstacle showing an acceleration to supercritical flow, a hydraulic jump and boundary-layer separation behind the maximum transverse dimension. (*b*) Hydrogen bubble picture of rearward wake when $T = 438$, $N = 6{\cdot}58$.